Identification of Ubiquitin Ligase From Grapevine Ring C3H2C3E3 and Characterization of Drought Resistance Function of VyRCHC114

Yihe Yu
Henan University of Science and Technology
Shengdi Yang
Henan University of Science and Technology
Lu Bian
Henan University of Science and Technology
Keke Yu
Henan University of Science and Technology
Xiangxuan Meng
Henan University of Science and Technology
Guohai Zhang
Henan University of Science and Technology
Weirong Xu
Ningxia University
Wenkong Yao
Ningxia University
Dalong Guo (guodalong@haust.edu.cn)
College of Forestry, Henan University of Science and Technology, Luoyang, 471023, Henan Province, China; 2 Henan Engineering Technology Research Center of Quality Regulation and Controlling of Horticultural Plants, Luoyang, 471023, Henan Province, China. https://orcid.org/0000-0001-5379-5255

Research article

Keywords: RING, drought stress, grapevine, ubiquitin, overexpression

Posted Date: August 27th, 2020

DOI: https://doi.org/10.21203/rs.3.rs-52911/v1

Abstract

Background: RING is one of the largest E3 ubiquitin ligase families and C3H2C3 type is the largest subfamily of RING, playing an important role in plants' development and growth and their biotic and abiotic stress responses.

Results: A total of 143 RING C3H2C3-type genes (*RCHCs*) were discovered from the grapevine genome and separated into groups (I-XI) according to their phylogenetic analysis, with these genes named according to their positions on chromosomes. Gene replication analysis showed that tandem duplications play a predominant role in the expansion of *VyRCHCs* family together. Structural analysis showed that most *VyRCHCs*(67.13%) had no more than 2 introns, while genes clustered together based on phylogenetic trees had similar motifs and evolutionarily conserved structures. Cis-acting element analysis showed the diversity of *VyRCHCs* regulation. The expression profiles of eight DEGs in RNA-Seq after drought stress were similar to those in qRT-PCR analysis. The in vitro ubiquitin experiment showed that *VyRCHC114* had E3 ubiquitin ligase activity, overexpression of VyRCHC114 in Arabidopsis improved drought tolerance, moreover, the transgenic plant survival rate increased by 30%, accompanied by changing of electrolyte leakage, chlorophyll content and the activities of SOD, POD, APX and CAT were changed. *AtCOR15a*, *AtRD29A*, *AtERD15* and *AtP5CS1* were expressed quantitatively, the results showed that they participated in the drought stress response may be regulated by the expression of *VyRCHC114*.

Conclusions: Valuable new information on the evolution of grapevine *RCHCs* and its relevance for studying the functional characteristics of grapevine *VyRCHC114* genes under drought stress emerged from this research.

Background

To survive in a changing environment, post-translational modification of proteins often occurs when plants perceive and transmit internal or external signals. The acetylation, methylation, phosphorylation, and ubiquitination of proteins are the main types of post-translational modification, which play a key role in different plant development stages and plant-environment interactions. The process of classifying intracellular proteins under the action of a variety of special enzymes, and specifically modifying the screened target proteins, is called ubiquitination [1]. In eukaryotic cells, the ubiquitin system is complex and mainly involves ubiquitin (a small molecule protein), an intact 26S proteasome, and ubiquitin-activating enzyme (E1), ubiquitin-binding enzyme (E2), and ubiquitin-ligase (E3) [2]. The inactivated ubiquitin-dependent ATP is first activated by E1 through the thioester bond formed between the C-terminal of ubiquitin and the cysteine residue of E1; then the ubiquitin signal connected to E1 is transferred to the acetylcysteine of E2. In the next step, the ubiquitin linked to E2 is transferred directly or indirectly to the lysine residue of the target protein via E3. It is noteworthy that E3 ubiquitin ligase is the main factor which determines the specific protein binding during ubiquitination [3], in that it can repeatedly add ubiquitin to the substrate protein, so that eventually the target protein is degraded by the 26S protease [4].

In recent years, mounting research has shown that the RING E3 ligase gene also figure prominently in abiotic stress responses of plants [5]. *SpRing* is a RING-type E3 ubiquitin ligase located in endoplasmic reticulum and participates in salt stress signal transmission in wild tomato variety *Solanum pimpinellifolium* 'PI365967'. In addition, *SpRing* is silenced by virus-induced gene silencing, resulting in increased sensitivity of wild tomato to salt stress. Overexpression of *Arabidopsis thaliana* in spring can improve its salt tolerance [6]. *SDIR1* (SALT- AND DROUGHT-INDUCED REALLY INTERESTING NEW GENE FINGER1) is a RING-type E3 ubiquitin ligase that regulates the salt stress response and ABA signaling in Arabidopsis by degrading the target protein SDIRIP1 (SDIR1-INTERACTING PROTEIN1). The downstream transcription factor ABI5 (ABA-INSENSITIVE5) is regulated by SDIRIP1, and overexpression of ABI5 increases salt tolerance [7]. The E3 ubiquitin ligase *OsHTAS* (*Oryza sativa* HEAT TOLERANCE AT SEEDLING STAGE), which regulates the stomatal opening state in the leaves by regulating ROS homeostasis, thus improving the basal heat resistance of the leaves. It involves two pathways, aba dependent and dst-mediated [8]. In Arabidopsis, *CHYR1* (CHYZINC-FINGERANDRINGPROTEIN1) encodes the RING-type E3 ubiquitin ligase which interacts with a related protein kinase KINASE2 (SnRK2) and can be phosphorylated by SnRK2.6 on its Thr-178 residues. When mediated by ABA, CHYR1 promotes the production of reactive oxygen species (ROS), stomatal closure, and drought tolerance in plants [9]. The capsicum annular E3 ubiquitin ligase, *CaAIRF1* (*Capsicum annuum* ADIP1 INTERACTING RING FINGER PROTEIN1), can interact with protein phosphatase *CaADIP1* and positively regulate ABA signaling pathway to improve drought tolerance [10]. In *Zea mays*, *ZmXerico1* encodes a RING-type E3 ligase, which can regulate the stability of ABA8'-hydroxylase protein and thereby enable control of the dynamic balance of ABA; hence, expression of *ZmXerico1* endows maize plants with ABA sensitivity and improves their water use efficiency under drought stress [11]. Furthermore, Arabidopsis *AtAIRP1*, *AtAIRP2*, *AtAIRP3* and *Capsicum annuum* CaAIR1 jointly encode a E3 ubiquitin ligase, by regulating ABA signaling transduction to regulate drought responses, the expression of these genes increases ABA-mediated stomatal closure [12–15]. Collectively, the above studies suggest E3 ligase is crucial for responding to abiotic stress.

Grapevine (*Vitis vinifera* L.) is a major cash crop, whose cultivated varieties have a total worldwide output of nearly 70 million tons of the fruit berries from more 7 million hectares of harvested land [16]. This plant is mainly grown to produce table grapes, fruit juices, and wine [17]. Most grapevine producing areas in the world incur seasonal droughts. According to global climate modeling, droughts will intensify in the near future. Drought can adversely affect the growth and development of grapevines, because under drought stress the concentration of cytokinin in their stems decreases, vegetative and reproductive growth is inhibited [18]. When a grapevine is in full bloom, drought stress will also affect its pollination process, which decreases the fruit setting rate and affects the size of the individual fruit berries produced [19]. With worsening water shortages, drought stress may well become a key factor impacting grapevine and wine production worldwide [20]. Therefore, it is of great significance to grapevine production and breeding to study the drought resistance of wild grapevine plants as this could uncover the molecular mechanisms enabling them to withstand drought effects. *Vitis yeshanensis* is a wild grapevine plant native to arid areas of China, whose morphological characteristics indicate adaptability to arid

environments in many aspects [21]. Several studies have shown that wild *Vitis yeshanensis* has stronger drought resistance than other cultivars [22, 23].

Although the RING-type gene family has been found in more and more plant species, and its importance for plants' stress responses and growth and development increasingly recognized, RING-type genes have yet to be fully identified in grapevine. The RING type E3 ubiquitin ligase is reportedly involved in grapevine's stress and growth, but too few studies have investigated E3 ubiquitin ligase's involvement in the regulation of grapevine response to drought stress. This study aimed to characterize the RING-type E3 ubiquitin ligase in grapevine's genome and its relevance for drought stress. To do this, genome-wide identification of C3H2C3 genes, the largest subfamily of grapevine RING-type, was carried out, coupled to their phylogenetic analysis, gene structure analysis, chromosome mapping, gene replication analysis, and cis-acting element analysis in gene promoter regions. We also quantified the expression levels of these genes under simulated drought treatment, and obtained a group of DEGs. The *VyRCHC114* gene was confirmed by RT-qPCR, and then the ubiquitin ligase activity of this gene verified. The functioning of this gene under drought conditions was elucidated using Arabidopsis transgenic plants. Our study provides an important basis for ubiquitin regulation of drought stress in grapevine.

Results

Genome-wide identification of RING C3H2C3 type finger proteins in grapevine

The results of the Hidden Markov Model (HMM) were analyzed, and the gene sequences were extracted and given to SMART, CDD, and Pfam for domain authentication. From this, 143 *VyRCHC* genes were obtained by comparing and screening genes with eight conservative metal ligands, and the alignment members were not abandoned. The physicochemical properties of each of the 143 *VyRCHCs* were identified (Table 1). The number of amino acids encoded by the 143 *VyRCHCs* ranged from 70 (*VyRCHC50*) to 763 (*VyRCHC98*). For these genes, the molecular weights of their products varied from 7.83 kDa to 83.58 kDa, while their isoelectric points varied from 3.88 to 9.95.

Analysis of VyRCHCs in the C3H2C3 domain

The typical RING domain is considered to be an octahedral group of metal-bound cysteine and its residues, which can chelate two zinc ions in a spherical cross-supported structure, in which the metal ligands 1 and 3, and 2 and 4, each bind to one zinc ion. This structure, however, requires a certain distance between adjacent metal ligands, it being variable between ml2 ~ ml3 and ml6 ~ ml7. We calculated statistics for this distance between adjacent metal ligands (Table S2). It was found that, except those between ml2 ~ ml3 and ml6 ~ ml7, the distances between other metal ligands were constant, while those from ml2 to ml3 spanned 11 to 24 amino acids, and for ml6 ~ ml7 the distance varied from 8 to 14 amino acids. The 143 *VyRCHCs* C3H2C3 domains have two amino acids between ml1 ~ ml2 and ml5 ~ ml6, while ml3 ~ ml4 contains one amino acid, ml7 ~ ml8 contains two amino acids

as does ml4 ~ ml5. To understand whether these RING C3H2C3 structural domains are conserved apart from their eight special metal ligands, their comparative analysis was conducted (Fig. S1). This revealed that some amino acids in the structural domain of RING C3H2C3 have a typical position bias (Fig. 1a). In the C3H2C3 type RING region, the ml2 located in front of amino acid residues is the most common Ile (I) or Val (V); likewise, the phenylalanine (Phe, F) residue is typically before ml5, the leucine residue (Leu, L) is always next to ml2, and the aspartic acid (Asp, D) residue is usually positioned after ml6, while the tryptophan residue (Trp, W) is usually the fourth following ml6. Notably, a very conservative proline (P) was found situated after ml7. According to the RING-type C3H2H3 domain schematic diagram, two pairs of metal ligands bind to a zinc ion (Fig. 1b). The total amino acid length of the C3H2C3 domain per *VyRCHC* gene and the corresponding number of different lengths were calculated: the vast majority of these were 41 and 42, accounting for 88.8% of all genes (Fig. 1c).

Phylogenetic analysis of VyRCHCs

To infer the evolutionary relationships of grapevine's *VyRCHCs*, Phylogenetic analysis of RCHC protein sequences of Arabidopsis, tomato, and grapevine were constructed (using the Maximum Likelihood method). According to the phylogenetic analysis, these 180 genes could be divided into 6 subgroups: ~ (Fig. 2). Group has the least number of members, only 12, and the group with the largest number of members is group , while the *RCHC* gene of *Arabidopsis thaliana* or tomato is found in each group. It is worth noting that more *RCHC* genes of *Arabidopsis thaliana* and tomato are gathered in group . Most of the RING-type C3H2C3 genes of grapevine display some homology to *RCHC* genes of Arabidopsis or tomato. In addition, in different groups, some gene pairs showed high similarity, which were confirmed in the distance of evolutionary relationship, the location of RING conserved domain and the length of protein sequence. For instance, *SlATL33* and *VyRCHC62*, *SlATL46* and *VyRCHC108*, *SlATL51* and *VyRCHC110*, *AtBRH1* and *VyRCHC116*, *AtRHA1A* and *VyRCHC13*, *AtSDIR1* and *VyRCHC97*, *AtRHC1A* and *VyRCHC59* etc. Next, a phylogenetic tree containing only 143 VyRCHC protein sequences was constructed (using the NJ method). To facilitate their study and analysis, the 143 members were divided into 11 groups (I ~ XI) according to the classification and phylogenetic analysis of Fig. S2, from which 27 pairs of genes with high homology were found. Based on their color-coded names, the *VyRCHCs* were then divided into six groups according to the number of conserved amino acids in their protein sequence.

Characterization of the motifs and gene structure of VyRCHCs

To further understand the diversity in motif composition between *VyRCHCs*, the MeMe analysis of VyRCHC proteins from groups I to XI was carried out. From this, 12 conserved motifs were identified in the VyRCHC protein, respectively named motif 1 to motif 12 (Fig. 3b), in which motif 1 and motif 2 is found in almost every *VyRCHCs*, this motif combines to form the eight most important metal ligand (Cys-Cys-Cys-His-His-Cys-Cys-Cys) structures of every *VyRCHC* gene. Importantly, there are 13 such structures in some genes, such as PA, CUE, DUF1117, zinc_ribbon_9, and zf-CHY, among others. These structures domain could be relevant for the function of *VyRCHCs*. The sequence information of motif 1 ~ 12 is presented in Table 2 (motif data). We next analyzed the exons, introns, and several key structures of *VyRCHCs*

(Fig. 3c). Most *VyRCHCs*(67.13%) had no more than 2 introns, with a maximum of 19 introns in *VyRCHC29* and none intron in 57 *VyRCHCs* (Fig. S3). The longest intron length was found in *VyRCHC141*.

According to the phylogenetic analysis of *VyRCHCs* (Fig. 3a), 45 pairs of genes can be found in the evolutionary tree. The results of the MeMe and gene structure analyses of these gene pairs were also similar (Fig. 3b and Fig. 3c). For example, the conserved motifs in the protein sequences of *VyRCHC44/64* are highly similar, and the gene's structure type and length are also similar, such as for *VyRCHC94/95, VyRCHC38/97, VyRCHC18/78, VyRCHC28/67* and *VyRCHC11/107*, to name a few. Unexpectedly, the MeMe analysis of *VyRCHC22/23/24, VyRCHC55/127, VyRCHC105/133*, and *VyRCHC13/116* gene pairs gave near identical results to those from the gene structure analysis, revealing a remarkably similar protein sequence length, gene structure length and the intron number among them. We thus speculate these four gene pairs may perform similar functions in grapevine plants.

Chromosomal localization and gene replication analysis of VyRCHCs

According to the location of *VyRCHCs* in the grapevine genome, 143 *VyRCHCs* were placed on 20 chromosomes (Fig. 4a), albeit unevenly distributed among them. Imprinting of the *VyRCHCs* was found in each chromosome of grapevine, but the number of genes on different chromosomes varied. The most found were 12 *VyRCHCs* on chromosome 11, the 11 *VyRCHCs* were identified on chromosome 1,7,13 and 18. Further, we also observed that these most of these *VyRCHCs* are likely distributed at both ends of the chromosome, leaving only a small portion of them in its middle part. Gene replication events include tandem replication and segmental replication, both of which are very vital for expanding the number of members of the gene family. To clarify the amplification mechanism of *VyRCHCs* during their evolution, we studied their potential repetitive events of *VyRCHCs*. According to the intraspecific alignment of 143 *VyRCHCs*, 9 pairs of genes, 7 and 2, were respectively identified as associated with tandem or segmental replication events. Among the 9 pairs of gene events, the tandem repeat frequency between chromosomes 1 was the highest, there were six tandem replication events, moreover, one pair of genes on chromosomes 3 identified as tandem replication genes, These results suggested that the main replication event mode of grapevine *VyRCHCs* family is via tandem replication; hence, it could have played a crucial role in the amplification of *VyRCHCs* during their evolutionary history.

To explore the selection of grapevine *VyRCHCs* in terms of their repetition and differentiation, the non-synonymous (Ka), synonymous (Ks), and Ka/Ks of each duplicated *VyRCHCs* were calculated. Among the 9 pairs of repetitive genes in grapevine, the Ka/Ks values of one pair were all less than 0.5, while the average Ka/Ks value was 0.325. It is worth noting that 8 pairs had Ka/Ks values less than 0.5, indicating that most of the repeated grapevine *VyRCHCs* were under negative selection during evolution (Table 3). Figure 4b shows that grapevine, Arabidopsis, and tomato all retained similar *RCHC* genes in their evolutionary history. It is worth noting the absence of homologous genes with *VyRCHC29* in tomato, but their presence in Arabidopsis, which may have arisen from gene deletions in the process of evolution, given that the same genes are *VyRCHC11*, *VyRCHC38*, *VyRCHC107*, *VyRCHC119*, and *VyRCHC137*. Nonetheless, two or more *RCHC* genes in Arabidopsis and tomato were found homologous to one

VyRCHC gene; for example, *VyRCHC89* and *Solyc07g053850.3/Solyc12g005470.2* and *AT4G28370/AT2G20650*, as well as those of *VyRCHC1*, *VyRCHC32*, *VyRCHC97*, *VyRCHC104*, *VyRCHC118*, and *VyRCHC142*. Hence, these genes may be parallel gene pairs and the putative source of amplifications of *RCHC* genes during evolution.

Cis-acting element analysis in VyRCHCs promoter

To further investigate the transcriptional regulation of *VyRCHCs*, cis-acting elements in the 2000 bp region upstream of the *VyRCHCs*' codon were predicted. The predicted cis-acting elements can be divided into seven categories according to their functions: namely, light response (32), hormone response (11), growth and development response (9), stress response (6), enhanced promoter cis-acting (6), binding site cis-acting (6), and other functional cis-acting (2) elements. Most promoters of grapevine *VyRCHCs* contained the CAAT-box or TATA-box, which are involved in the enhanced promoter cis-acting elements. In addition, 127 *VyRCHCs* promoters harbored the stress response element ARE, more than half of the promoters of the *VyRCHCs* having the hormone response elements ABRE, TGACG-motif, CGTCA-motif, and over half of the *VyRCHCs* also featured the G-box, GT1-motif, and Box 4 in their promoters (Table S3). In the 2000 kb region upstream of *VvRCHCs*, discovered very many different functions of cis element, in addition to the common cis element with light response and enhanced the promoter, also found that the more growth and adversity stress related cis element, this suggests that *VyRCHCs* may widely participating in various life activities of plant.

It is known that the RING gene can play a key role in plants' growth and response to abiotic stresses. Accordingly, the cis-acting elements related to abiotic stress, growth and hormone regulation were focused upon here. The respective locations of the five major acting elements associated with hormone response, binding sites, growth and development, and stress of our concern, on the promoter of the *VyRCHCs* (Fig. S4a) were determined. To accurately identify the stress-related elements, we focused on four kinds (anaerobic induction, injury response, low temperature, drought response (Fig. S4b), low temperature response, defense and stress response), whose locations are also depicted. In addition, we counted the number of major elements related to stress, growth and development, and hormone responses in the *VyRCHC* gene promoter (Fig. S4b). Evidently, concerning growth and development, the number of O2-sites is the largest, there are 5 promoters of *VyRCHC6* and 4 promoters of *VyRCHC40*. In terms of stress, the number of ARE is very large, found in 89% of the *VyRCHCs* promoters, moreover, 5 of the most promoters of *VyRCHC14* and *VyRCHC81* occurred. In terms of hormone response, the number of ABRE is dominant, found in 64% of the *VyRCHCs* promoters, moreover, 9 of the most promoters of *VyRCHC3* and *VyRCHC16* occurred. Surprisingly, 22 of the *VyRCHC74* gene promoters were found and 11 of the *VyRCHC128* gene promoters were found. These results suggested that *VyRCHCs* may be associated with cis-acting elements of different functions; in other words, these genes may be regulated by these elements and thereby influence related plant life activities.

Expression analysis of VyRCHCs in roots of two grapevine rootstocks with different drought sensitivity

To investigate differential *VyRCHCs*' expression between plants having contrasting drought-resistant genes (101.14 vs. M4) under drought stress and their potential functioning, the grapevine RNA-Seq transcriptome database of the published dataset was used [24]. We checked the expression of 143 *VyRCHCs*; of them, 7 *VyRCHCs* were not expressed at any time, so we excluded them.

To understand the expression of these *VyRCHCs* under the drought treatment, we used the ratio of WS (Water Stress) to WW (Well-Watered) gene expression of the two genotypes to draw an expression heat map, expression values are reported as log2 of the fold change (WS/WW) fold change. (Fig. 5a), the differential multiple matrixes of these *VyRCHCs* is recorded in Table S4. However, more than 60% of the *VyRCHCs* in the two genotypes were highly expressed under the imposed drought. To screen out the key genes, in each time period of the treatment, the gene that conforms to $|\log2 (WS/WW)| > 1$ is considered a differential gene, and the Venn diagram was made using the differentially screened genes of the drought-tolerant genotype M4 at different times (Fig. 5b). By looking at the different genes in each period, there are finally 8 genes that are different in three periods. To robustly verify the gene expression levels, we quantified the expression levels of these 8 key genes (Fig. 6), whose pattern basically conformed to the trend shown in Fig. 5c. That is, the *VyRCHC114* gene was significantly down-regulated at 2 days, with a strong downward trend through 4, 7, and 10 days of the drought treatment. The *VyRCHC66*, *VyRCHC68*, *VyRCHC69* and *VyRCHC95* genes had a similar expression trend, being slightly up-regulated at 2 days of drought, but strongly down-regulated at 4, 7, and 10 days thereafter. These results suggested eight key genes are probably involved in regulating the plant response to drought.

Identification of E3 ubiquitin ligase activity of VyRCHC114

To clarify whether *VyRCHC114* has E3 ubiquitin ligase activity, we conducted an in vitro ubiquitin activity assay, achieved by using purified MBP-*VyRCHC114* fusion protein mixed with ubiquitin, E1, and E2 and by western blotting with the MBP antibody. Ubiquitin molecules were detected on the fusion protein linked by MBP antibody (Fig. 7a). This same method was used to detect ubiquitin antibody tags. The *VyRCHC114* protein was detected in the fusion protein linked by the ubiquitin antibody, which indicated it had E3 ligase activity.

We knew the RING-C3H2C3 type protein can form a RING structure for ubiquitin regulation, but this process depends on the interaction between the eight conserved metal ligands. To further illustrate whether and how E3 ligase activity of *VyRCHC114* depends on these conserved metal ligands, as shown in Fig. 7c, we selected four different amino acid sites for mutation (two key conservative and two non-conservative metal ligand sites). Four corresponding proteins (C320S, C328S, H341A, N355A) were obtained, and their ubiquitin activity in vitro was tested by the same method. After the immuno-blotting analysis of MBP antibody and ubiquitin antibody, evidently the two mutant proteins C320S and H341A lost their E3 ubiquitin ligase activity due to mutations at key sites, but the two mutant proteins C328S and N355A maintained theirs (Fig. 7b). These results indicated these conserved metal ligand sites are crucial factors for demonstrating the *VyRCHC114*'s ligase activity.

Overexpression of VyRCHC114 enhances Arabidopsis drought tolerance

To clarify the effects of *VyRCHC114*'s role in plant responses to drought, we selected transgenic Arabidopsis (OE #2, #5, #13) with high expression levels of the *VyRCHC114* gene for subsequent experiments (Fig. 8b). After 15 days of drought imposed upon wild plants and transgenic plants, followed by normal watering for 6 days, phenotype observations revealed plants overexpressing *VyRCHC114* had significantly improved the drought tolerance (Fig. 8a). Further, on average, more than 70% of the plants overexpressing *VyRCHC114* survived the drought stress, which was significantly higher than the 30% survival of the EV-transformed group (Fig. 8c).

To understand the relationship between plant growth and drought resistance, electrolyte leakage rate (Fig. 9a) and chlorophyll content (Fig. 9b) were both measured. These were similar between *VyRCHC114*-overexpressed and EV-transformed plants in the non-stress treatment, but after 8 days of drought stress, the electrolyte permeability of the former was significantly lower than the latter's, while the chlorophyll content was significantly higher in overexpressing than EV-transformed plants. Additionally, the changes in photosynthesis under drought stress were further analyzed by measuring potential photosynthetic efficiency (Fig. 9c) and capacity storage capacity (Fig. 9d). Each was not significantly different between EV-transformed and *VyRCHC114* overexpression plants when they were non-stressed; however, Fv/Fm was significantly higher in the latter than the former at 4 days, and especially at 7 days, of drought stress. At 4 days, energy storage capacity of *VyRCHC114*-overexpressed plants was not significantly different from that of EV-transformed plants, but at 7 days of drought stress, that of the former exceeded the latter. Hence, these results suggested *VyRCHC114* could enhance the drought resistance of plants by participating in the regulation of photosynthesis.

Moreover, much research has shown that antioxidant enzymes can influence plants' drought tolerance. Common antioxidant enzymes are ascorbate peroxidase (APX), superoxide dismutase (SOD), peroxidase (POD), and catalase (CAT), so we examined their activity. As Fig. 10 shows, under non-stress conditions, the activity of these antioxidant enzymes was similar between the plants, whereas when drought stressed for 4 and 7 days, the activities of APX (Fig. 10a), SOD (Fig. 10b), POD (Fig. 10c) and CAT (Fig. 10d) were significantly higher in plants overexpressing *VyRCHC114* than those EV-transformed. Taken together, these data indicate *VyRCHC114* may also improve drought tolerance by elevating antioxidant enzyme activity.

AtCOR15a, *AtERD15*, *AtP5CS1*, and *AtRD29A* are known to be key genes for regulating plant responses to drought stress, so we quantified their expression under imposed drought. As expected, when non-stressed, there was no significant difference between plants overexpressing *VyRCHC114* overexpression and those EV-transformed. By contrast, under drought stress, all four genes were significantly higher in *VyRCHC114*-overexpressed plants than in those EV-transformed (Fig. 11).

Discussion

The RING C3H2C3 gene family has since been identified in many plant species [25–28]. Related studies have shown that RING genes are involved in a variety of biological processes, growth and development

and hormonal responses, as well as plant responses to abiotic stresses [29]. However, for grapevine, the RING C3H2C3 gene had not yet been identified in its whole genome, with few reports available on its relevance for grapevine's growth and developmental regulation or response to abiotic stress. In our study, we analyzed the whole genome of grapevine for the RING C3H2C3 gene family members. Using the criteria of whether the eight conserved metal ligands are present, a total of 143 non-redundant RING C3H2C3 genes were thus identified. Studies have shown that grapevine's genome size is about 0.5 times that of tomato, containing 0.75 times as many genes as tomato [30, 31]. According to the known RING C3H2C3genes in tomato, the genes account for 0.58 in grapevine, which lies between the multiples of genome length and the number of genes [26].

Many RING C3H2C3 of E3 ubiquitin ligases belong to the ATL gene family [32]. According to Arabidopsis and tomato RING C3H2C3 genes. we divided grapevine's RING C3H2C3 genes into six categories (~) (Fig. 2). Each group has Arabidopsis or tomato in the same branch. This shows that grapevine genes have sequence similarity with *Arabidopsis thaliana* and tomato genes. Our evolutionary analysis of grapevine, Arabidopsis, and tomato provided evidence that the replication events of these genes occurred after their retention during the differentiation from common ancestors before species differentiation. Gene replication can arise from fragment replication, tandem replication, transposable events and even whole genome replication, which not only provide the evolutionary potential for species to produce new functional traits but also are a main driving force for species differentiation [33, 34]. In the identification of gene families from many species, gene replication events have proven instrumental in their expansion [35]. We observed that some grapevine *VyRCHCs* correspond to one or more intraspecific homologous genes, thus indicating *VyRCHC* gene family's amplification in this plant may have been caused by gene duplication. Studies have shown that tandem replication often occurs in widely and fast evolving gene families, a good example being Nucleotide Binding Sites Leucine Rich Repeat (NBS-LRR) resistance families [36]. Segmental replication is more common in slow evolving gene families, like the MYB gene family [36]. We found 7 of 2 pairs of RING-type C3H2C3 genes participated in segmental replication (Fig. 4). Therefore, a finding consistent with other grapevine gene families, like the WRKY family genes in the autopolyploid *Saccharum spontaneum* [37]. We calculated the Ka/Ks values of 9 pairs of repetitive genes in grapevine (Table 3), finding that repeated *VyRCHCs* were in a strong state of purification and selection in their evolution, with an average Ka/ Ks of 0.395.

Cis-acting elements in gene promoter regions may be critical for gene regulation. The DELLA protein and its interacting RING finger protein inhibit the gibberellin response, by binding to the promoter of a subset of the gibberellin response gene in Arabidopsis [38]. Analysis of cis-acting elements in grapevine's *VyRCHCs* revealed the existence of different types of cis-acting elements upstream of the C3H2C3 genes. Except for a large number of components related to optical responses, plant hormone regulation, growth and development, and stress were also common upstream of different *VyRCHCs*. This situation is in fact rather common in RING genes of all species [25–28]. Ubiquitin ligase SDIR1 regulates stress-responsive abscisic acid signal by interacting with ABRE abscisic acid response element [39]. ABA, GA, ethylene, trauma, drought, heat stress, and pathogen response elements are present in the promoter region of *OsRING* genes of rice plants, for which pathogen infection, SA, ABA, JA, and ethephon (ET) treatments

could induce target genes expression to different degrees [40]. A similar analysis of RING C3H2C3 gene *mRHCP1* was recently done in maize [41]. Therefore, we speculate that these *VyRCHCs* may be involved in a variety of different regulatory mechanisms through these cis-acting elements.

According to the analysis of RNG-Seq data set (Fig. 5a), more than 60% of *VyRCHCs* were significantly up-regulated or down-regulated under drought stress, indicating those genes may play a key role in how grapevine responds to drought. Studies have revealed the molecular mechanism of many circular genes involved in the drought stress. For example, in Arabidopsis, *XERICO, SDIR1, AtAIRP1, AtAIRP2, AtAIRP3* and *AtAIRP4* has been found to play a key role in the drought response of plants. In addition, an E3 ubiquitin ligase *atrzf1* mutation increased the proline content of Arabidopsis and improved this plant's drought tolerance [42]. Similarly *GpDSR7* encodes an E3 ubiquitin ligase, which when overexpressed in Arabidopsis increased its tolerance to drought stress [43]. In our study, and according to previous screening methods [44], we focused on genes which were significantly up-regulated or down-regulated at four time periods during the drought treatment, as they more likely to play a key role in grapevine's drought stress response (Fig. 5b and 5c). Comparing the RNA-Seq dataset with the RT-qPCR data (Fig. 6), it was found that the *VyRCHC114* gene was significantly down-regulated within 2 days of experiencing drought, which continued to decline strongly through 10 days after this treatment. Hence, we postulated the *VyRCHC114* gene may possess E3 ubiquitin ligase activity enabling it to participate in the regulation of grapevine drought stress responses. Verifying this, we detected that *VyRCHC114* has E3 ubiquitin ligase activity and the *VyRCHC114* gene is overexpressed in Arabidopsis. Some related indexes of Arabidopsis plant fitness under drought stress were observed. That experiment demonstrated that the survival rate of overexpressed plants and the activities of many antioxidant enzymes were significantly increased. Drought stress significantly inhibited the greater electrolyte permeability of overexpressed plants; correspondingly, the decreasing trend of chlorophyll content was eliminated, while reductions in photosynthetic efficiency and energy storage capacity were significantly inhibited.

Drought stress greatly impacts the photosynthesis of plants, by affecting their photosynthetic rates and carbon metabolic pathways[45]. A lowered rate of photosynthesis can lead to excessive accumulation of reactive oxygen species (ROS), leading to cytotoxicity, membrane lipid peroxidation, and even cell death [46, 47] which can be countered by antioxidant enzymes as a form of plant defense. The overexpression of maize E3 ubiquitin ligase gene in transgenic tobacco can reportedly improve the drought resistance of tobacco [48]. Not only that, other abiotic stresses may also be regulated by photosynthesis, thus enabling plants to adapt to stress conditions [49]. According to our results, *VyRCHC114* overexpressing plants maintained a strong photosynthetic rate and energy storage capacity while under drought stress. The reason for this may be an increase of their chloroplast content, pointing to *VyRCHC114*'s possible involvement in the regulation of chlorophyll biosynthesis pathway as an E3 ubiquitin ligase. Nonetheless, we also examined the expression of genes known to play a major role in drought stress responses of plants [50–52]. Our results revealed that the expression levels of these genes were significantly higher in *VyRCHC114*-overexpressed than EV-transformed Arabidopsis *plants*. Moreover, antioxidant system may be involved in plant abiotic stress tolerance mediated by the E3 ubiquitin ligase. Here, we provide physiological evidence that *VyRCHC114* heterologous expression enhances drought resistance by

increasing the activity of antioxidant enzymes, which can scavenge for and eliminate ROS to indirectly reduce membrane damage.

Conclusions

VyRCHC may act as an E3 ligase to mediate substrate degradation through the ubiquitin proteasome mechanism. This interaction may cause the target protein to be labeled by ubiquitin signaling, which leads to proteasome degradation. Since *VyRCHC114* likely represents a new class of positive /negative regulatory factors in the drought signal pathway, however, positive/negative depends on the regulatory characteristics of the target protein, but we think the degraded protein is a positive regulator of drought signaling, so that more of this substance may activate drought signaling. Therefore, *VyRCHC114* may improve the water retention ability and antioxidant defense of plants by regulating their chlorophyll content and antioxidant system, thus participating in drought stress response. So far, however, the target protein of the plant *VyRCHC114* gene has not been determined, nor is the mechanism of augmented SOD, POD, APX and CAT activities clearly understood. In future work, we will focus on the identification of *VyRCHC114* target proteins under drought stress and activation mechanisms of the antioxidant system in *VyRCHC114*-transgenic plants.

Methods

Plant materials

The grapevine variety *Vitis yeshanensis* was sampled from the field, located in the grape germplasm resource garden of Northwest A&F University. Annual plants are selected for treatment, and the treatment method is the same[53]. Root samples were taken at 0d, 2d, 4d, 6d, 8d and 10d respectively for subsequent experiments. Transgenic and wild type (WT) plants of *Arabidopsis thaliana* ecotype Columbia (Col-0) plants were grown in vermiculite: perlite (1:1, v/v) mix in plastic pots in a growth chamber. Arabidopsis plants were grown in a soil mix of peat moss, perlite, and vermiculite (3:1:1, v/v/v) under a 12-h/12-h day/night cycle at 25°C with 60% relative humidity. For the drought stress treatment, plants were transformed with an empty vector (EV) or to overexpress *VyRCHC114* (OE#2, OE#5, or OE#13 lines) [54], all of which were grown on individual MS medium plates for 7 days before transplantation into soil, there were 5 strains in the control and three transgenic lines. This experiment mainly followed previous research methods, albeit slightly modified [55]. After 3 weeks, these plants received a 12-day drought stress treatment (no water provided), after which they were re-watered and their survival recorded 6 days later. All experiments were repeated three times.

Identification of RING-type C3-H2-C3 genes in the grapevine genome

To identify the C3H2H3 type of RING, the most recent grapevine genome file in the Ensembl Plants Database (http://plants.ensembl.org/index.html) was downloaded and used. The grapevine RING

C3H2C3 candidates were identified based on the HMM profiles (PF13639 and PF12678) with an e-value cutoff of 0.01. The screened proteins screened were given to Pfam (http://pfam.xfam.org/search/) and SMART (ttp://smart.embl-heidelberg.de/), e value less than 0.01. Finally, 143 genes were confirmed as RING C3H2C3 genes, after manually checking whether their protein sequences had eight definite metal ligands (Cys-Cys-Cys-His-His-Cys-Cys-Cys). The physicochemical properties of each RING-type C3H2C3 protein were predicted using the Protparam online tool (https://web.expasy.org/protparam/). The 143 *VyRCHCs* were named according to their positional information on the chromosomes.

Bioinformatics analysis of VyRCHCs family

CLUSTALX 2.0 software was used to perform a multiple-sequence alignment of the 143 grapevine genes and the 20 tomato and 17 Arabidopsis RCHC protein sequences; it was also used to manually remove any untrusted gaps at both sequence ends. A phylogenetic tree was generated in MEGA 7.0 using the ML (maximum likelihood) method and bootstrapping with n = 1000 replicates, with all other settings set to their default values; the online EVOLVIEW (https://www.evolgenius.info/evolview/#login/) tool carried out the tree's visualization. The online program Gene Structure Display Server 2.0 (http://gsds.cbi.pku.edu.cn/) was used to identify the genetic structure the *VyRCHCs*. Using the MEME online program (http://MEME.nbcr.net/meme/introduction.html), the VyRCHC protein sequences could be analyzed under these parameters: an optimal motif width of 6 ~ 35 and a maximum number of motifs of 12. According to the annotated positions in grapevine genome data, the 143 grapevine *VyRCHCs* were located on 20 chromosomes. By referring to previous studies, BLASTN was used to compare the CDS sequences of *VyRCHCs* in grapevine and tomato (e-value = 1×10^{-10}, homology > 75%). The tandem repeat gene pairs and segment repeat gene pairs of *VyRCHCs* were also identified [56, 57]. Further, the Ka/Ks ratio between repetitive genes pairs can be used to infer the selection pressure in the process of genome evolution. Next, the MCScanX program was used to detect the collinear region between *VyRCHCs* in grapevine and tomato/Arabidopsis; any collinear gene pair of *VyRCHCs* was marked with red and green lines. The cis-elements were identified from the upstream 2-kb promoter sequences of the *VyRCHCs* after submitting them to PlantCARE (http://bioinformatics.psb.ugent.be/webtools/plantcare/html) [58], to obtain their image display, the resulting XML file was uploaded to TBtools [59].

Expression analysis of VyRCHCs in grapevine under drought stress

To analyze the grapevine *RCHC* genes' expression levels under drought stress, we obtained from the NCBI database (registration number: SRA110531) two different drought resistance genes (101.14 and M4) which were compared under two different treatments WS(Water Stress) and WW (Well-Watered) in roots and in different periods (T1–T4:2d□4d□7d□10d) RNA-Seq data set. Based on the expression values of RING C3H2C3 in the roots of the two genotypes, we calculated the log2(WS/WW) values (fold-change) in each time period (Table S4). The R package 'pheatmap' was used to produce a heatmap for this data.

RNA extraction and quantitative real-time PCR (qRT-PCR)

The qRT-PCR primers were designed using Primer Premier 5 software. The RNA from Arabidopsis and grapevine (*Vitis yeshanensis*) leaves was extracted using the Spectrum Plant Total RNA Kit (Sigma-Aldrich, Beijing, China), after which reverse transcription of RNA into cDNA was done using the Prime Script RT Reagent Kit (Takara, Dalian, China). The qRT-PCR was performed in an IQ^5 real-time PCR detection system (Bio-Rad Laboratories, Hercules, CA, USA) with SYBR Premium EX Taq II (Takara, Dalian, China). The reaction volume was 25 μl. The relative expression level corresponding to *β-TUB4* gene was calculated by using the $2^{-\Delta\Delta Ct}$ method [60]; each reaction was prepared in triplicate and repeated three times. Primer sequence information in Table S1.

E3 ubiquitin ligase activity assay

The open reading frame (ORF) of VyRCHC114 and the different site mutants C320S, H341A, C328S, and N355A were separately cloned into the SalI/KpnI site of the pMAL-c5X vector (New England Biolabs UK Ltd, Hitchin, UK). According to the manufacturer's instructions, the pMAL protein fusion and purification system (New England Biolabs) was used to purify the fusion protein. Ubiquitination activity was then measured that according to the method described above [61], albeit with the following modifications made: 250 ng of purified E3 (MBP-*VyRCHC114*, C320S, H341A, C328S, and N355A) in the ubiquitination buffer (50 mM Tris-HCl (pH 7.5), while the other reagents and steps used were the same. Primer sequence information in Table S1.

Physiological analysis of drought stress response of transgenic Arabidopsis

To determine the water loss rate, 10 leaves were detached from 3-week-old transgenic and WT plants and immediately weighed. The samples were then placed on dry filter paper at a relative humidity of 40–45% at room temperature and weighed over a time course. Leaves were sampled after dehydration to detect cell death, electrolyte leakage, malondialdehyde, antioxidant enzyme activity. The leaves collected before dehydration were used as a negative control.

For chlorophyll content measurements, approximately 0.05 g of fresh leaf material was placed in 5 ml of 96% ethanol and incubated at 4◦C in the dark overnight. The absorbance of the extracted pigments was measured at 665 and 649 nm using a spectrophotometer (Hitachi Limited, Tokyo, Japan) and the chlorophyll content was calculated as previously described[53].

Relative electrolyte leakage was measured as previously described [62], as was MDA content [61]. In addition, superoxide dismutase (SOD), peroxidase (POD), catalase (CAT), ascorbate peroxidase (APX) enzyme activities were extracted from 0.5 g leaves from abiotic stress treated plants as well as control plants, and measured as described by [63].

Statistical analysis

All the above experiments by SPSS version 21.0 was employed to analyze the statistically significant differences of the gene expression levels by ANOVA with Duncan's multiple range test. All experiments

were repeated three times as independent analyses.

Abbreviations

RCHCs, RING C3H2C3-type genes; DEGs, differentially expressed genes; qRT-PCR, quantitative real-time reverse transcription PCR; RNA-seq, RNA-sequencing; WS, Water Stress; WW, Well-Watered; ML, Maximum Likelihood; WT, wild type; HMM, Hidden Markov Model.

Declarations

Ethics approval and consent to participate

Not applicable.

Consent for publication

Not applicable.

Availability of data and materials

All data generated and analyzed during this study are included in this published article. To identify the C3H2H3 type of RING, the most recent grapevine genome file in the Ensembl Plants Database (http://plants.ensembl.org/index.html) was downloaded and used. Expression data of C3H2H3 type of RING genes in grapevine used in this study can be accessed via the NCBI SRA database with accession numbers of SRA110531. Figure S1 Schematic diagram of C3H2C3 conserved protein sequence alignment of VyRCHCs. Figure S2 Phylogenetic analysis of RCHC protein in grapevine. Figure S3 Number of introns in *VyRCHCs*. Figure S4 Analysis of cis-acting elements in the *VyRCHCs*. Table S1 The sequences of the primers used in these experiments. Table S2 The distance between conserved metal ligands in the C3H2H3 domain of 143 VyRCHCs. Table S3 Functions of the cis-acting elements that found in the promoter region of each of *VyRCHCs*. Table S4 Differential multiple expression matrix of *VyRCHCs*.

Competing interests

The authors have no conflict of interest to report.

Funding

This work was financially supported by grants from the Natural Science Foundation of China (no. NSFC:31701893 and U1504321), Zhongyuan Science and Technology Innovation Leaders (no. 194200510007), and Innovative Research Team in Henan University of Science & Technology, China (no. 2015TTD003). The Funding bodies were not involved in the design of the study and collection, analysis, and interpretation of data and in writing the manuscript.

Authors' contributions

Y.H.Y. and S.D.Y. conceived the original screening and research plans. S.D.Y. performed most of the experiments and finished the writing of the paper. D.L.G. participated in the modification of the paper L.B., K.K.Y., X.X.M. and G.H.Z. assisted in sorting out the data. W.R.X. and W.K.Y. provided guidance for experiments. Y.H.Y. and S.D.Y. wrote the article with contributions of all the authors. All authors read and approved the final manuscript.

Acknowledgements

We would like to thank all the colleagues in our laboratory for providing useful discussions and technical assistance.

References

1. Sadanandom A, Bailey M, Ewan R, Lee J, Nelis S. The ubiquitin–proteasome system: central modifier of plant signalling. New Phytol. 2012;196(1):13–28.
2. Sharma B, Joshi D, Yadav PK, Gupta AK, Bhatt TK. Role of ubiquitin-mediated degradation system in plant biology. Front Plant Sci. 2016;7:806.
3. Kelley DR. E3 Ubiquitin Ligases: Key Regulators of Hormone Signaling in Plants. Mol Cell Proteomics. 2018;17(6):1047–54.
4. Stone SL. The role of ubiquitin and the 26S proteasome in plant abiotic stress signaling. Front Plant Sci. 2014;5:135.
5. Shu K, Yang W. E3 Ubiquitin Ligases: Ubiquitous Actors in Plant Development and Abiotic Stress Responses. Plant Cell Physiol. 2017;58(9):1461–76.
6. Qi S, Lin Q, Zhu H, Gao F, Zhang W, Hua X. The RING Finger E3 Ligase SpRing is a Positive Regulator of Salt Stress Signaling in Salt-Tolerant Wild Tomato Species. Plant Cell Physiol. 2016;57(3):528–39.
7. Zhang H, Cui F, Wu Y, Lou L, Liu L, Tian M, Ning Y, Shu K, Tang S, Xie Q. The RING finger ubiquitin E3 ligase SDIR1 targets SDIR1-INTERACTING PROTEIN1 for degradation to modulate the salt stress response and ABA signaling in Arabidopsis. Plant Cell. 2015;27(1):214–27.
8. Liu J, Zhang C, Wei C, Liu X, Wang M, Yu F, Xie Q, Tu J. The RING finger ubiquitin E3 ligase OsHTAS enhances heat tolerance by promoting H2O2-induced stomatal closure in rice. Plant Physiol. 2016;170(1):429–43.
9. Ding S, Zhang B, Qin F. Arabidopsis RZFP34/CHYR1, a ubiquitin E3 ligase, regulates stomatal movement and drought tolerance via SnRK2. 6-mediated phosphorylation. Plant Cell. 2015;27(11):3228–44.
10. Lim CW, Baek W, Lee SC. The pepper RING-type E3 ligase CaAIRF1 regulates ABA and drought signaling via CaADIP1 protein phosphatase degradation. Plant Physiol. 2017;173(4):2323–39.
11. Brugière N, Zhang W, Xu Q, Scolaro EJ, Lu C, Kahsay RY, Kise R, Trecker L, Williams RW, Hakimi S. Overexpression of RING domain E3 ligase ZmXerico1 confers drought tolerance through regulation of ABA homeostasis. Plant Physiol. 2017;175(3):1350–69.

12. Ryu MY, Cho SK, Kim WT. The Arabidopsis C3H2C3-type RING E3 ubiquitin ligase AtAIRP1 is a positive regulator of an abscisic acid-dependent response to drought stress. Plant Physiol. 2010;154(4):1983–97.
13. Cho SK, Ryu MY, Seo DH, Kang BG, Kim WT. The Arabidopsis RING E3 ubiquitin ligase AtAIRP2 plays combinatory roles with AtAIRP1 in abscisic acid-mediated drought stress responses. Plant Physiol. 2011;157(4):2240–57.
14. Kim JH, Kim WT. The Arabidopsis RING E3 ubiquitin ligase AtAIRP3/LOG2 participates in positive regulation of high-salt and drought stress responses. Plant Physiol. 2013;162(3):1733–49.
15. Park C, Lim CW, Baek W, Lee SC. RING Type E3 Ligase CaAIR1 in Pepper Acts in the Regulation of ABA Signaling and Drought Stress Response. Plant Cell Physiol. 2015;56(9):1808–19.
16. Yu Y, Bian L, Yu K, Yang S, Zhang G, Guo D. Grape (Vitis davidii) VdGATA2 functions as a transcription activator and enhances powdery mildew resistance via the active oxygen species pathway. Sci Hortic. 2020;267:109327.
17. Wang M, Vannozzi A, Wang G, Liang Y-H, Tornielli GB, Zenoni S, Cavallini E, Pezzotti M, Cheng Z-MM. Genome and transcriptome analysis of the grapevine (Vitis vinifera L.) WRKY gene family. Hortic Res. 2014;1:14016.
18. Hardie W, Considine J. Response of grapes to water-deficit stress in particular stages of development. Am J Enol Viticult. 1976;27(2):55–61.
19. dos Santos TP, Lopes CM, Rodrigues ML, de Souza CR, Maroco JP, Pereira JS, Silva JR, Chaves MM. Partial rootzone drying: effects on growth and fruit quality of field-grown grapevines (Vitis vinifera). Funct Plant Biol. 2003;30(6):663–71.
20. Chaves MM, Flexas J, Pinheiro C. Photosynthesis under drought and salt stress: regulation mechanisms from whole plant to cell. Ann bot. 2009;103(4):551–60.
21. Wan Y, Schwaninger H, Li D, Simon C, Wang Y, Zhang C. A review of taxonomic research in Chinese wild grapes. Vitis-Geilweilerhof. 2008;47(2):81.
22. Yang Y, He M, Zhu Z, Li S, Xu Y, Zhang C, Singer SD, Wang Y. Identification of the dehydrin gene family from grapevine species and analysis of their responsiveness to various forms of abiotic and biotic stress. BMC Plant Biol. 2012;12(1):140.
23. Jing Z, Wang X. Genetic relationship between Chinese wild Vitis species and American and European cultivars based on ISSR markers. Biochem Syst Ecol. 2013;46:120–6.
24. Corso M, Vannozzi A, Maza E, Vitulo N, Meggio F, Pitacco A, Telatin A, D'Angelo M, Feltrin E, Negri AS, et al. Comprehensive transcript profiling of two grapevine rootstock genotypes contrasting in drought susceptibility links the phenylpropanoid pathway to enhanced tolerance. J Exp Bot. 2015;66(19):5739–52.
25. Li Y, Wu B, Yu Y, Yang G, Wu C, Zheng C. Genome-wide analysis of the RING finger gene family in apple. Mol Genet Genomics. 2011;286(1):81.
26. Yang L, Miao M, Lyu H, Cao X, Li J, Li Y, Li Z, Chang W. **Genome-Wide Identification, Evolution, and Expression Analysis of RING Finger Gene Family in Solanum lycopersicum**. *Int J Mol Sci* 2019,

20(19).

27. Qanmber G, Yu D, Li J, Wang L, Ma S, Lu L, Yang Z, Li F. Genome-wide identification and expression analysis of Gossypium RING-H2 finger E3 ligase genes revealed their roles in fiber development, and phytohormone and abiotic stress responses. J Cot Res. 2018;1(1):1–17.
28. Alam I, Yang YQ, Wang Y, Zhu ML, Wang HB, Chalhoub B, Lu YH. Genome-wide identification, evolution and expression analysis of RING finger protein genes in Brassica rapa. Sci Rep. 2017;7:40690.
29. Hua Z, Vierstra RD. The cullin-RING ubiquitin-protein ligases. Annu Rev Plant Biol. 2011;62:299–334.
30. Jaillon O, Aury J, Noel B, Policriti A, Clepet C, Casagrande A, Choisne N, Aubourg S, Vitulo N, Jubin C. The grapevine genome sequence suggests ancestral hexaploidization in major angiosperm phyla. Nature. 2007;449(7161):463.
31. Consortium TG. The tomato genome sequence provides insights into fleshy fruit evolution. Nature. 2012;485(7400):635.
32. Serrano M, Parra S, Alcaraz LD, Guzmán P. The ATL gene family from Arabidopsis thaliana and Oryza sativa comprises a large number of putative ubiquitin ligases of the RING-H2 type. J Mol Evol. 2006;62(4):434–45.
33. Ren R, Wang H, Guo C, Zhang N, Zeng L, Chen Y, Ma H, Qi J. Widespread whole genome duplications contribute to genome complexity and species diversity in angiosperms. Mol Plant. 2018;11(3):414–28.
34. Moore RC, Purugganan MD. The early stages of duplicate gene evolution. Proc Nat Acad Sci USA. 2003;100(26):15682–7.
35. Wang N, Liu Y, Cong Y, Wang T, Zhong X, Yang S, Li Y, Gai J. Genome-Wide Identification of Soybean U-Box E3 Ubiquitin Ligases and Roles of GmPUB8 in Negative Regulation of Drought Stress Response in Arabidopsis. Plant Cell Physiol. 2016;57(6):1189–209.
36. Cannon SB, Mitra A, Baumgarten A, Young ND, May G. The roles of segmental and tandem gene duplication in the evolution of large gene families in Arabidopsis thaliana. BMC Plant Biol. 2004;4(1):10.
37. Li Z, Hua X, Zhong W, Yuan Y, Wang Y, Wang Z, Ming R, Zhang J. Genome-Wide Identification and Expression Profile Analysis of WRKY Family Genes in the Autopolyploid Saccharum spontaneum. Plant Cell Physiol. 2019;61(3):616–30.
38. Park J, Nguyen KT, Park E, Jeon J-S, Choi G. DELLA proteins and their interacting RING Finger proteins repress gibberellin responses by binding to the promoters of a subset of gibberellin-responsive genes in Arabidopsis. Plant Cell. 2013;25(3):927–43.
39. Zhang Y, Yang C, Li Y, Zheng N, Chen H, Zhao Q, Gao T, Guo H, Xie Q. SDIR1 is a RING finger E3 ligase that positively regulates stress-responsive abscisic acid signaling in Arabidopsis. Plant Cell. 2007;19(6):1912–29.
40. Meng XB, Zhao WS, Lin RM, Wang M, Peng YL. Molecular cloning and characterization of a rice blast-inducible RING-H2 type Zinc finger gene: Full Length Research Paper. DNA Seq. 2006;17(1):41–

8.

41. LI W, Qi S, LI W, YU Y, Meng Z. MENG Z: Characterization and expression analysis of a novel RING-HC gene, ZmRHCP1, involved in brace root development and abiotic stress responses in maize. J Integr Agr. 2017;16(9):1892–9.
42. Ju HW, Min JH, Chung MS, Kim CS. The atrzf1 mutation of the novel RING-type E3 ubiquitin ligase increases proline contents and enhances drought tolerance in Arabidopsis. Plant Sci. 2013;203:1–7.
43. Li M, Li Y, Zhao J, Liu H, Jia S, Li J, Zhao H, Han S, Wang Y. **GpDSR7, a novel E3 Ubiquitin ligase gene in Grimmia pilifera is involved in tolerance to drought stress in Arabidopsis**. *PloS One* 2016, 11(5).
44. Ji XR, Yu YH, Ni PY, Zhang GH, Guo DL. Genome-wide identification of small heat-shock protein (HSP20) gene family in grape and expression profile during berry development. BMC Plant Biol. 2019;19(1):433.
45. Teng K, Li J, Liu L, Han Y, Du Y, Zhang J, Sun H, Zhao Q. Exogenous ABA induces drought tolerance in upland rice: the role of chloroplast and ABA biosynthesis-related gene expression on photosystem II during PEG stress. Acta physiol plant. 2014;36(8):2219–27.
46. Apel K, Hirt H. Reactive oxygen species: metabolism, oxidative stress, and signal transduction. Annu Rev Plant Biol. 2004;55:373–99.
47. Park JJ, Yi J, Yoon J, Cho LH, Ping J, Jeong HJ, Cho SK, Kim WT, An G. OsPUB15, an E3 ubiquitin ligase, functions to reduce cellular oxidative stress during seedling establishment. Plant J. 2011;65(2):194–205.
48. Liu J, Xia Z, Wang M, Zhang X, Yang T, Wu J. Overexpression of a maize E3 ubiquitin ligase gene enhances drought tolerance through regulating stomatal aperture and antioxidant system in transgenic tobacco. Plant Physiol Biochem. 2013;73:114–20.
49. Le Hir R, Castelain M, Chakraborti D, Moritz T, Dinant S, Bellini C. At bHLH68 transcription factor contributes to the regulation of ABA homeostasis and drought stress tolerance in Arabidopsis thaliana. Physiol Plant. 2017;160(3):312–27.
50. Hsieh T, Li C, Su R, Cheng C, Tsai Y, Chan M. A tomato bZIP transcription factor, SlAREB, is involved in water deficit and salt stress response. Planta. 2010;231(6):1459–73.
51. Yu D, Zhang L, Zhao K, Niu R, Zhai H, Zhang J. VaERD15, a transcription factor gene associated with cold-tolerance in Chinese Wild Vitis amurensis. Front Plant Sci. 2017;8:297.
52. Ma L, Li Y, Chen Y, Li X. Improved drought and salt tolerance of Arabidopsis thaliana by ectopic expression of a cotton (Gossypium hirsutum) CBF gene. Plant Cell. 2015;124(3):583–98.
53. Hou H, Jia H, Yan Q, Wang X. Overexpression of a SBP-Box Gene (VpSBP16) from Chinese Wild Vitis Species in Arabidopsis Improves Salinity and Drought Stress Tolerance. Int J Mol Sci. 2018;19(4):940.
54. Yu Y, Bian L, Yu K, Yang S, Zhang G, Guo D. Grape (Vitis davidii) VdGATA2 functions as a transcription activator and enhances powdery mildew resistance via the active oxygen species pathway. Sci Hortic. 2020;267:109327.

55. Guo R, Qiao H, Zhao J, Wang X, Tu M, Guo C, Wan R, Li Z, Wang X. The Grape VlWRKY3 Gene Promotes Abiotic and Biotic Stress Tolerance in Transgenic Arabidopsis thaliana. Front Plant Sci. 2018;9:545.
56. !!!. INVALID CITATION !!!.
57. Ni P, Ji X, Guo D. Genome–wide identification, characterization, and expression analysis of GDSL-type esterases/lipases gene family in relation to grape berry ripening. Sci Hortic. 2020;264:109162.
58. Lescot M, Déhais P, Thijs G, Marchal K, Moreau Y, Van de Peer Y, Rouzé P, Rombauts S. PlantCARE, a database of plant cis-acting regulatory elements and a portal to tools for in silico analysis of promoter sequences. Nucleic Acids Res. 2002;30(1):325–7.
59. Chen C, Chen H, Zhang Y, Thomas H, Frank M, He Y, Xia R. **TBtools - an Integrative Toolkit Developed for Interactive Analyses of Big Biological Data**. *Mol Plant* 2020.
60. Livak KJ, Schmittgen T. Analysis of relative gene expression data using real-time quantitative PCR and the 2(-Delta Delta C(T)) Method. Methods. 2001;25(4):402–8.
61. Yu Y, Xu W, Wang J, Wang L, Yao W, Yang Y, Xu Y, Ma F, Du Y, Wang Y. The Chinese wild grapevine (Vitis pseudoreticulata) E3 ubiquitin ligase Erysiphe necator-induced RING finger protein 1 (EIRP1) activates plant defense responses by inducing proteolysis of the VpWRKY11 transcription factor. New Phytol. 2013;200(3):834–46.
62. Zhang L, Zhao G, Xia C, Jia J, Liu X, Kong X. A wheat R2R3-MYB gene, TaMYB30-B, improves drought stress tolerance in transgenic Arabidopsis. J Exp Bot. 2012;63(16):5873–85.
63. Chen R, Wu P, Cao D, Tian H, Chen C, Zhu B. Edible coatings inhibit the postharvest berry abscission of table grapes caused by sulfur dioxide during storage. Postharvest Biol Tec. 2019;152:1–8.

Tables

Due to technical limitations, table 1 to 3 is only available as a download in the Supplemental Files section.

Figures

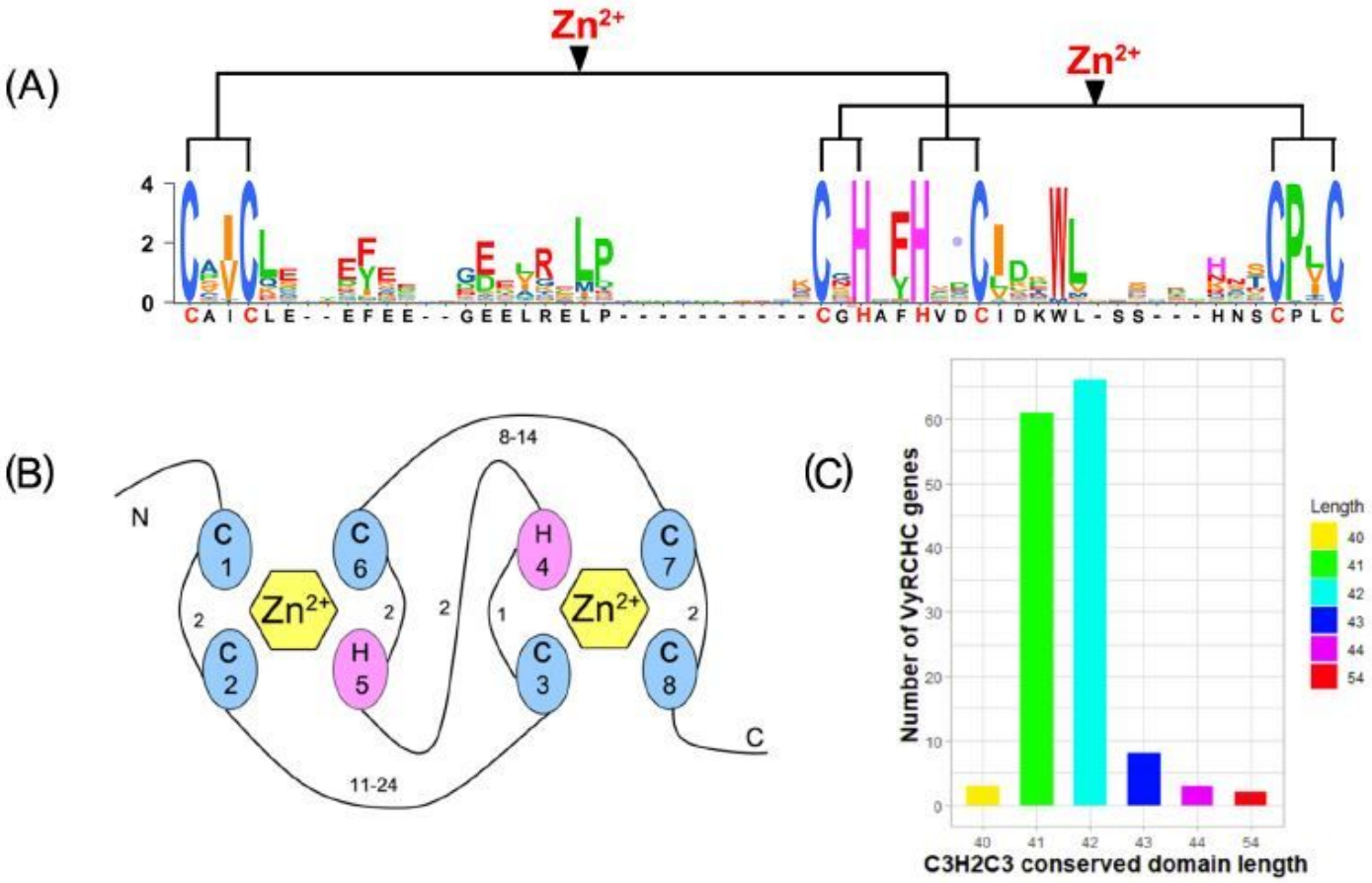

Figure 1

VyRCHCs' C3H2H3 domain analysis. a SeqLogo of VyRCHCs' C3H2H3 domain. b Schematic diagram of zinc ion binding to the C3H2C3 structure of the VyRCHCs. Cysteine and histidine are metal ligands marked numerically in ellipses. The hexagon represents a zinc ion. The number on the line between metal ligands is the number of amino acids between them. c The number of different amino acids in the VyRCHCs in the metal ligand region.

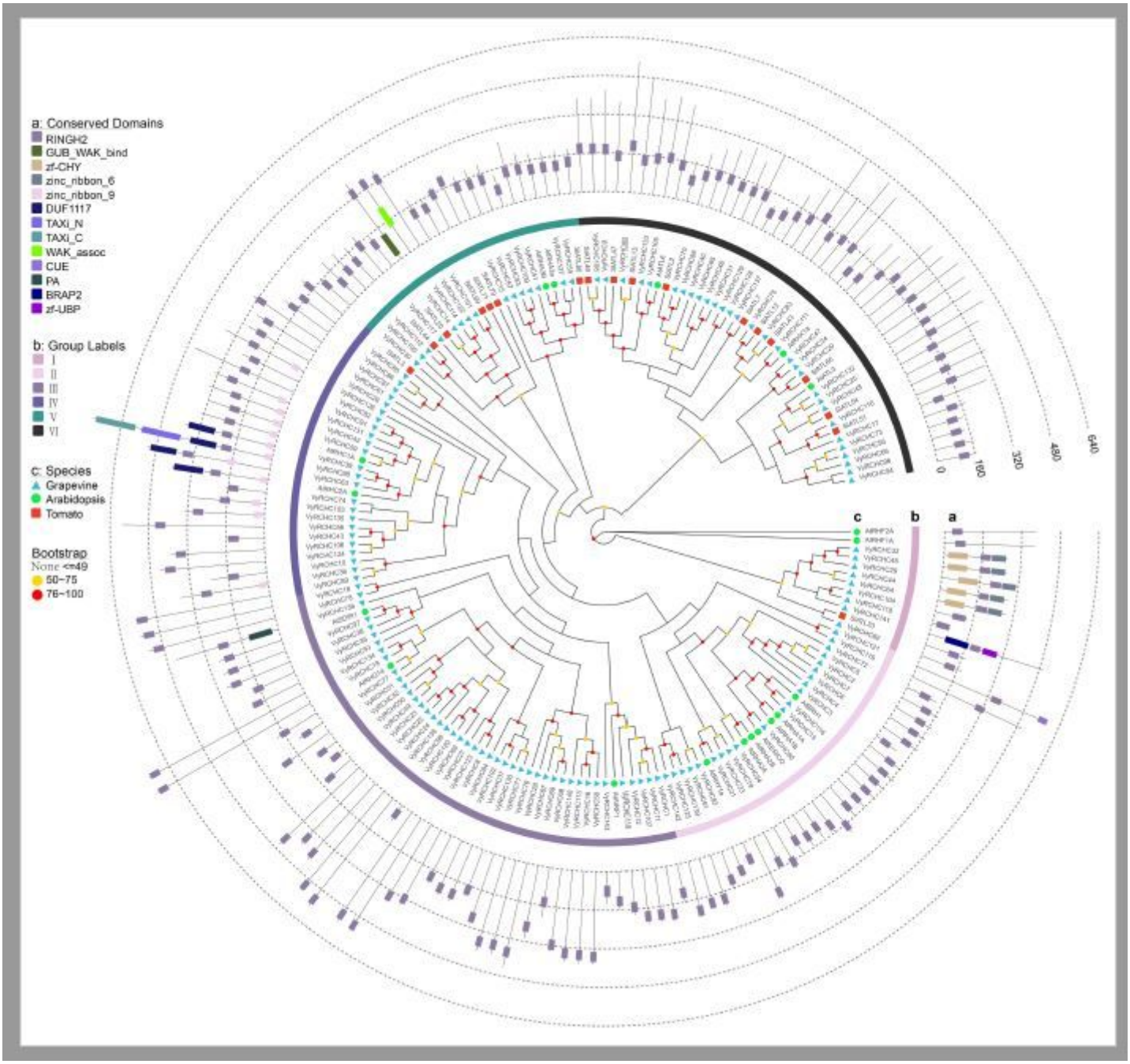

Figure 2

Phylogenetic analysis of RCHC protein in grapevine and other plants. Via the Maximum Likelihood method, MEGA7.0 was used to construct phylogenetic trees of grapevine, Arabidopsis, and tomato (Solanum lycopersicum) with RING-type C3H2H3 proteins. The number of bootstrap repeats was n = 1000. Displayed are the percentages of bootstrap scores greater than 50%. Conservative domains, grouping, and information on different species are shown in the form of a, b, c.

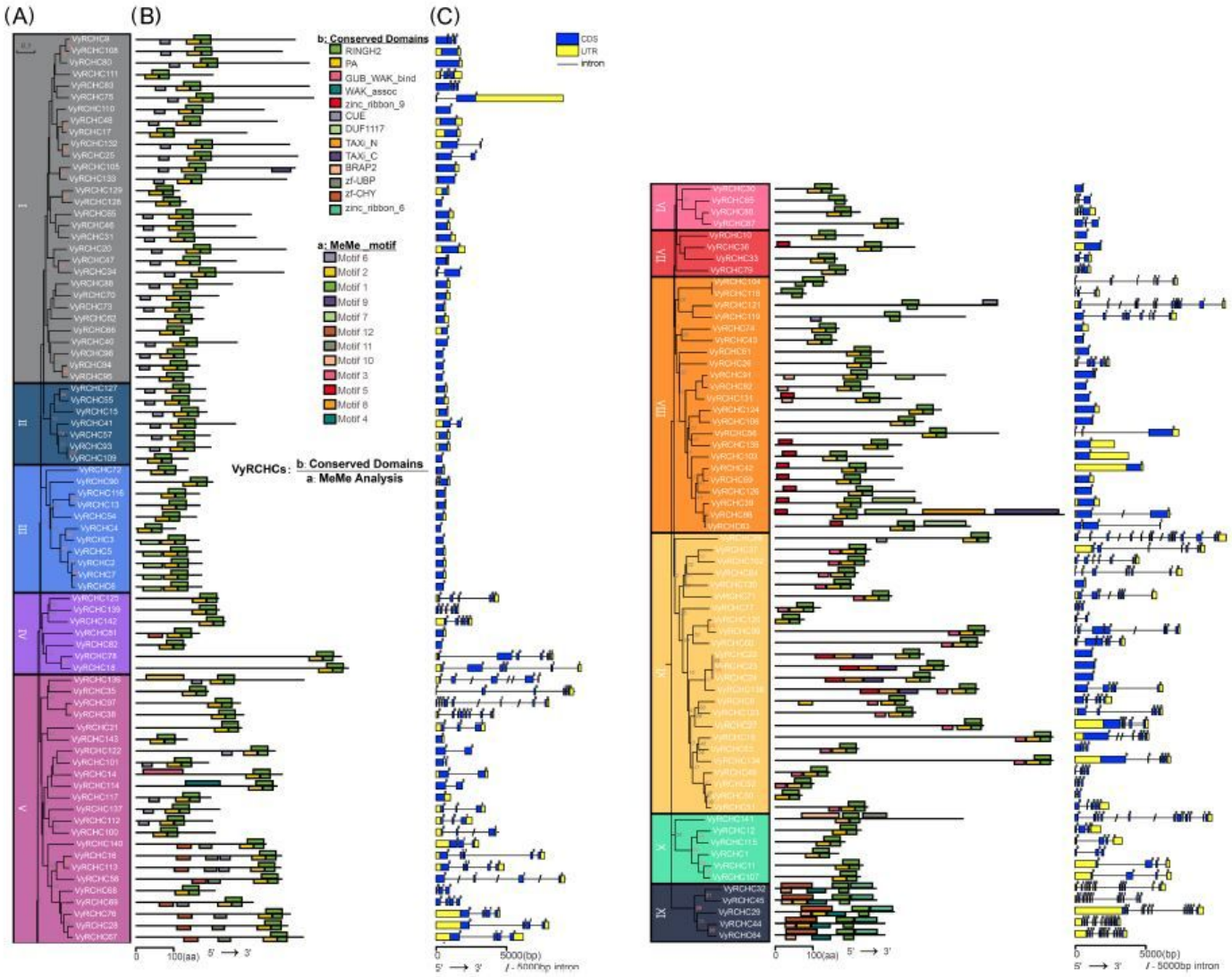

Figure 3

Phylogenetic tree, gene domain, and structure analysis of VyRCHCs in grapevine. a The phylogenetic tree of VyRCHCs was constructed using the NJ method. Different background colors represent different grouping branches. b Domain analysis of VyRCHCs proteins. At the bottom of the line, different colored squares represent different types of conserved amino acid sequences and based on MeMe analysis. The modules of different colors above the line represent the functional domains that have been identified. c Genetic structure of VyRCHCs, the CDS sequence is represented by a blue square/rectangle, the introns by black lines, the UTRs by yellow squares/rectangles.

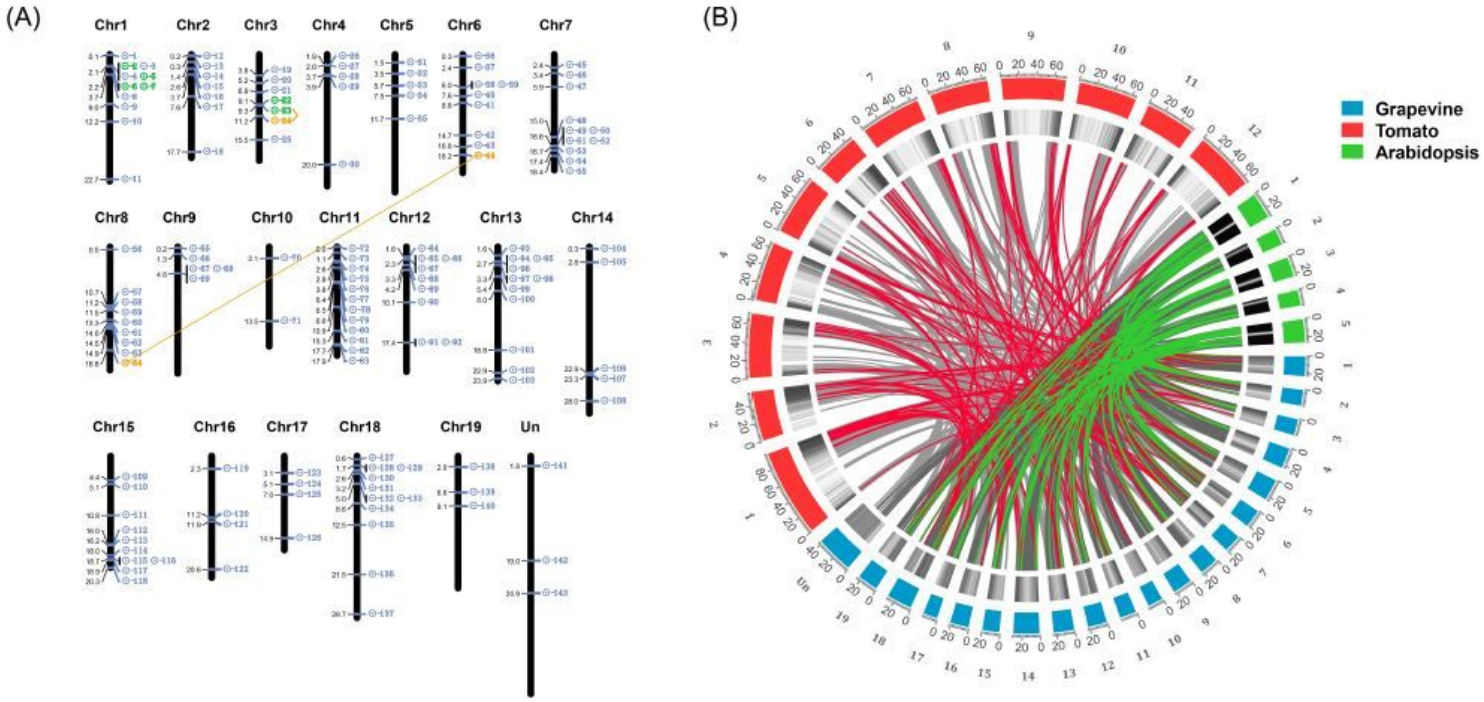

Figure 4

Chromosome location, gene replication, and collinear correlation. a Location information of VyRCHCs on grapevine chromosomes. Colored boxes and line connections represent the segmental repetitive gene pairs. b Collinear correlations of RCHCs in grapevine, tomato, and Arabidopsis. Each colored square is a chromosome (serial number). The black-and-white square shows the density of genes in each chromosome. Each line connects homologous genes; colored lines correspond to RCHCs, while gray lines denote other genes.

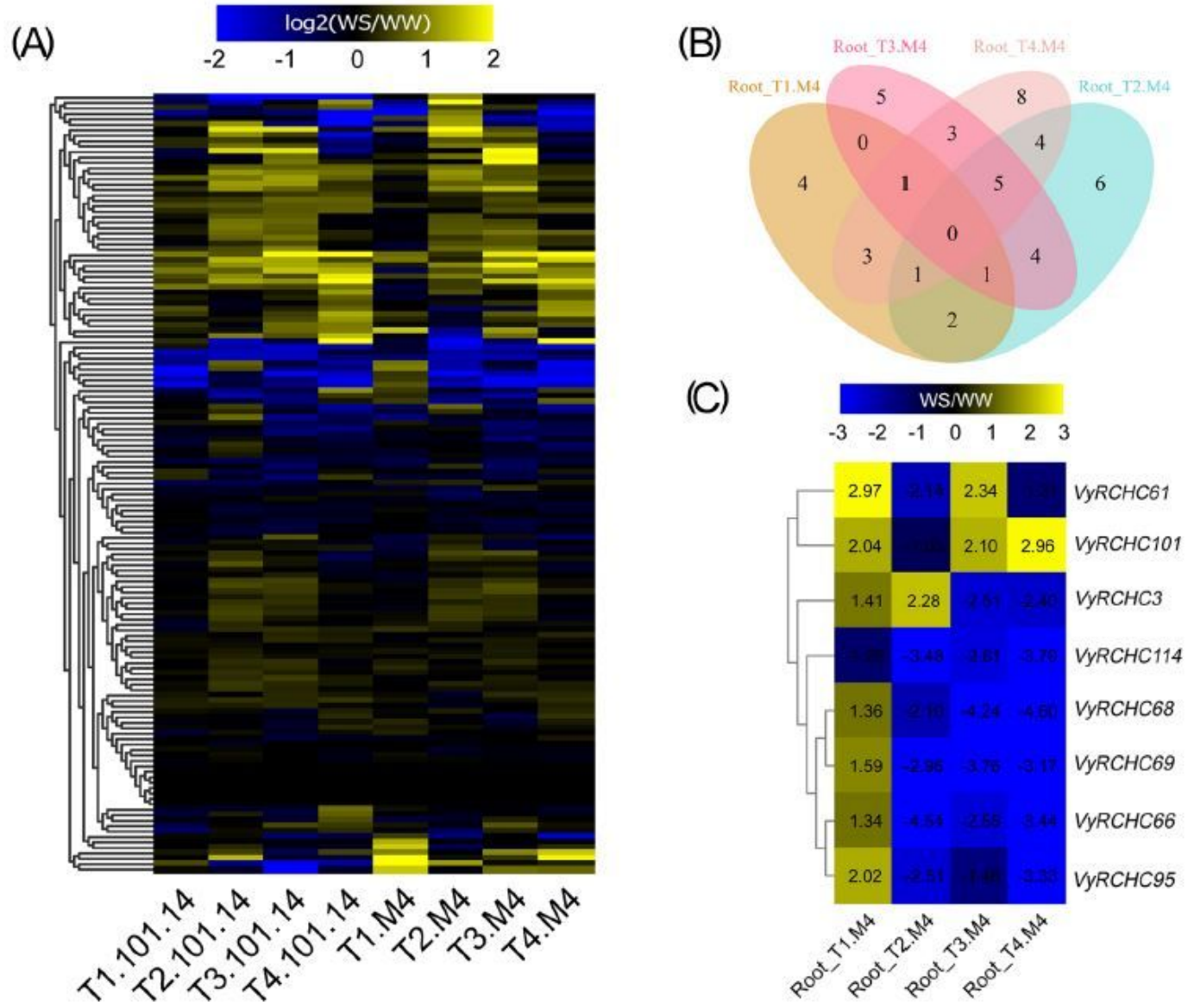

Figure 5

Differential heat map of VyRCHCs' expression in plants under drought stress conditions. a Heat maps of two different genotypes, based on their log2(WS/WW) values from the RNA-Seq data set, under drought stress and normal conditions at times T1–T4. b The Venn diagram of DEGs obtained from the analysis of the expression of M4 genotype at different periods. c Selected eight candidate genes in genotype M4 at different stages of WS/WW heat map.

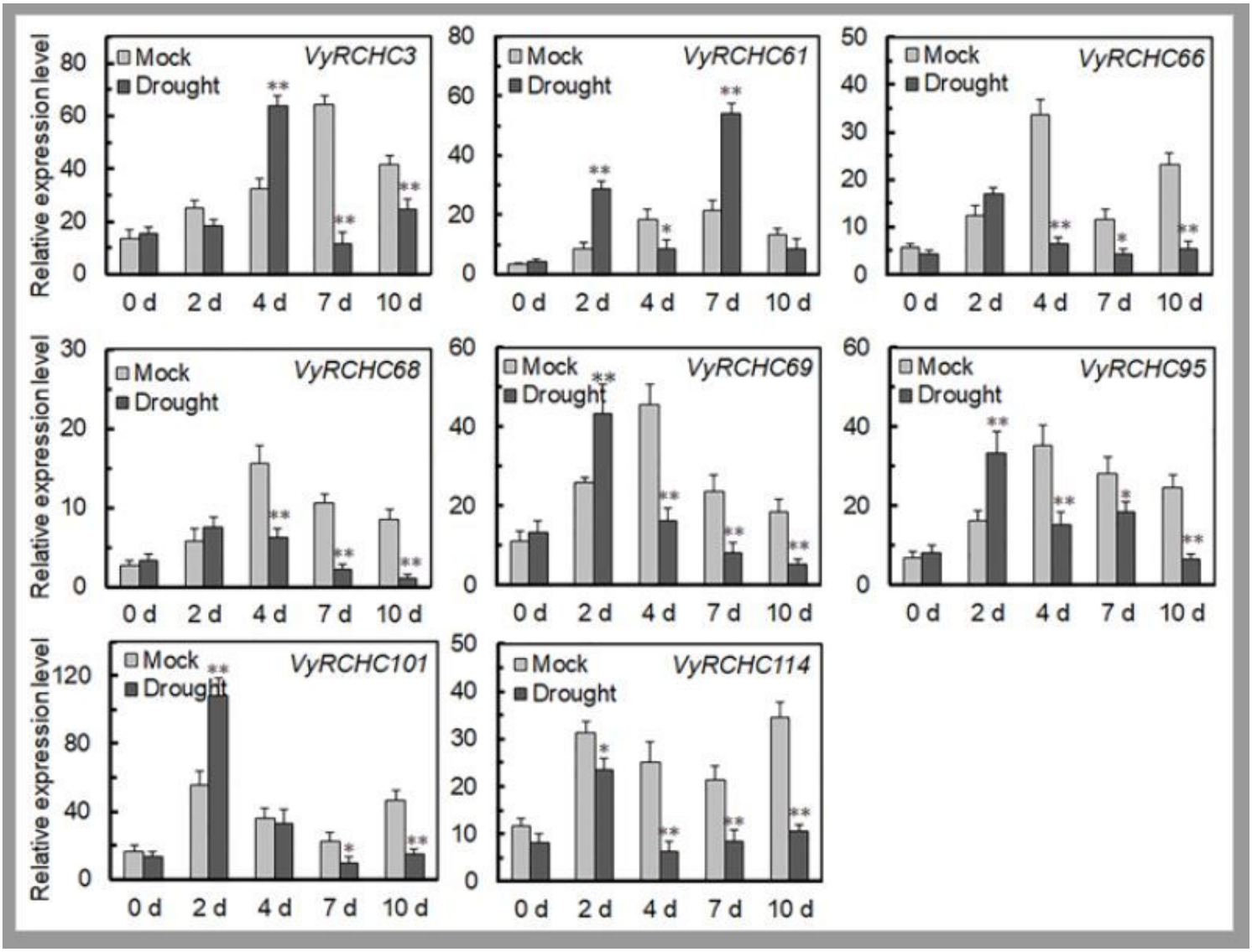

Figure 6

Expression of 8 candidate genes were screened in qRT-PCR for plants under drought stress and control conditions. The x-axis represents the different days during the treatment and the y-axis the relative levels of a gene's expression. Each treatment group had three biological repeats whose averages are plotted with the standard deviation. The asterisks indicate the significant level (* $P < 0.05$, ** $P < 0.01$).

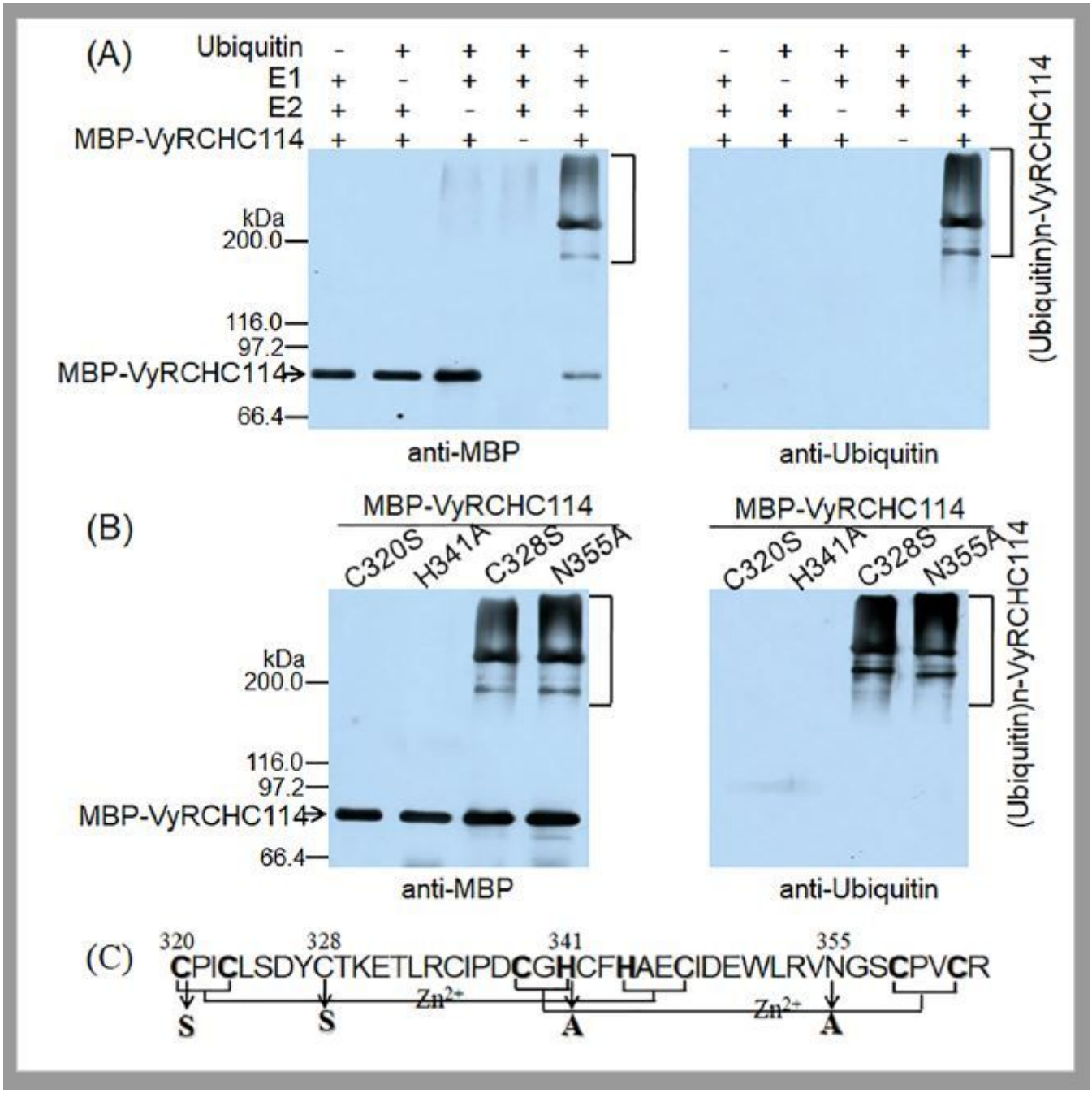

Figure 7

E3 ubiquitin ligase activity of VyRCHC114. a Determination of E3 ubiquitin ligase activity of VyRCHC114; an immunoblot analysis was performed with the ubiquitin antibody (right) and MBP antibody (left). b Determination of E3 ubiquitin ligase activity of VyRCHC114 mutants; an immunoblot analysis was performed with ubiquitin antibody (right) and MBP antibody (left). c Schematic diagram of VyRCHC114 C3H2C3 domain and putative mutation sites. C328S and N355A affect a non-conserved site of the VyRCHC114 C3H2C3 domain. Mutations in C320S and H341A affect the ubiquitin activity of VyRCHC114.

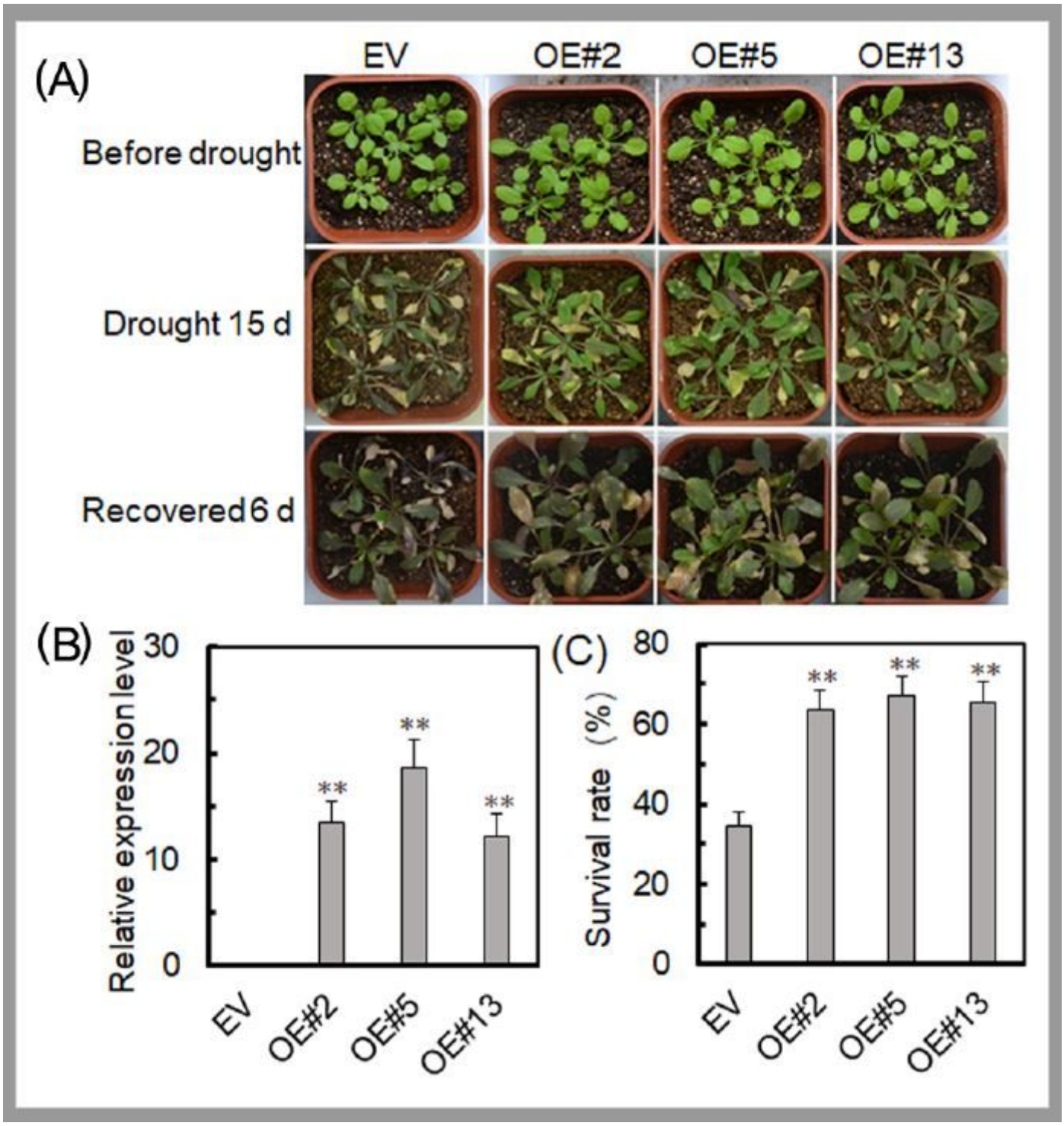

Figure 8

VyRCHC114 overexpression (OE) enhances drought resistance in Arabidopsis. a Phenotypes of three transgenic and an EV-transformed Arabidopsis lines after 15 days of drought stress and a 6-day recovery period. b,c Relative expression levels of VyRCHC114 and survival of transgenic and EV-transformed Arabidopsis plants. Data are the mean ± SD (standard deviation). The asterisk, (*) and (**), indicate that OEs and EV-transformed groups were significantly different at $P < 0.05$ and $P < 0.01$ (Student's t-test).

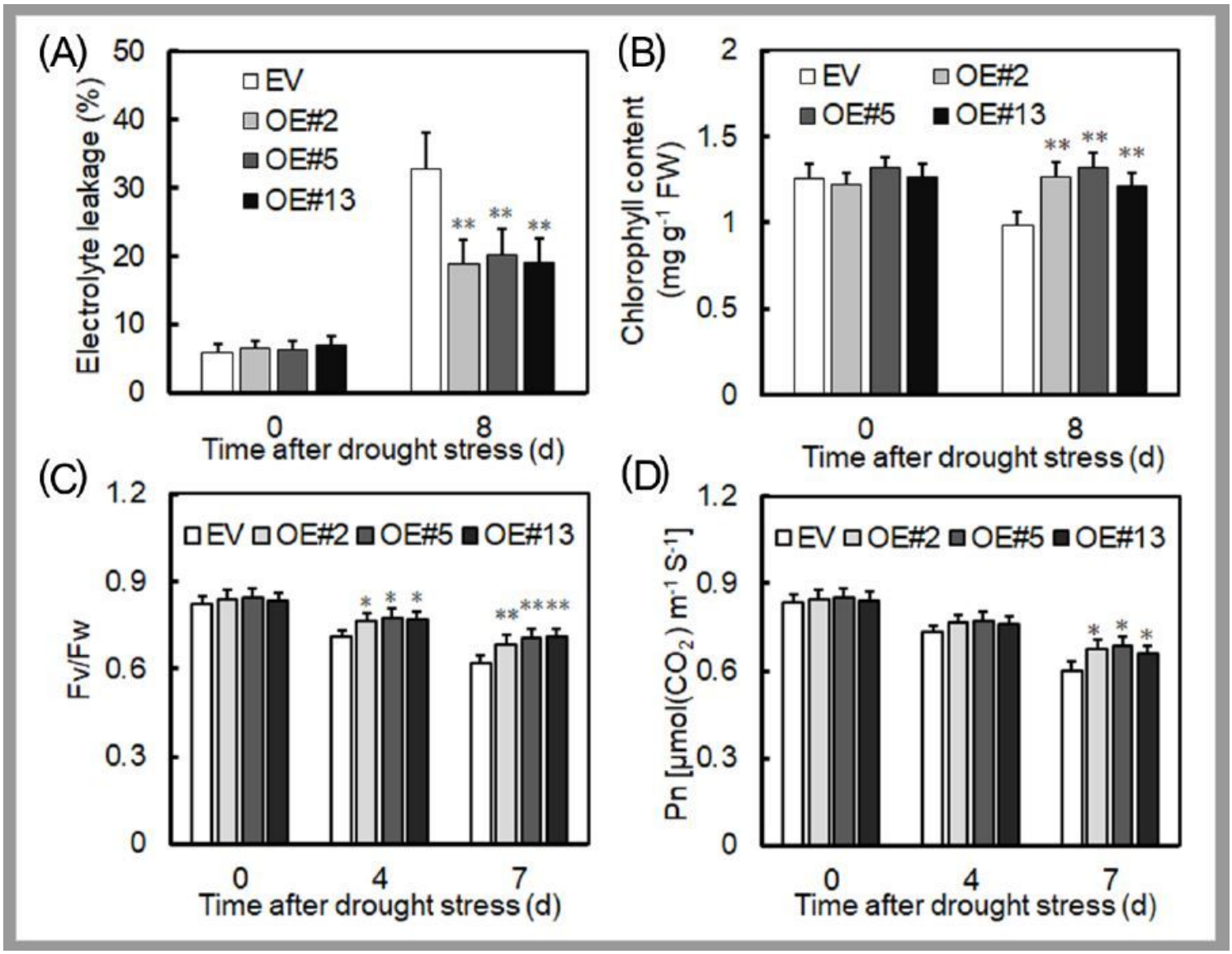

Figure 9

Physiological indices of the EV-transformed and overexpressing (OE) Arabidopsis plants after drought stress. a Electrolyte leakage, b chlorophyll content, c PSII maximal photochemical efficiency (Fv/Fm), d net photosynthetic rate of leaves (Pn) were evaluated. Data are the mean ± SD (standard deviation). The asterisk, (*) and (**), indicates that OEs and EV-transformed groups were significant different at $P < 0.05$ and $P < 0.01$ (Student's t-test).

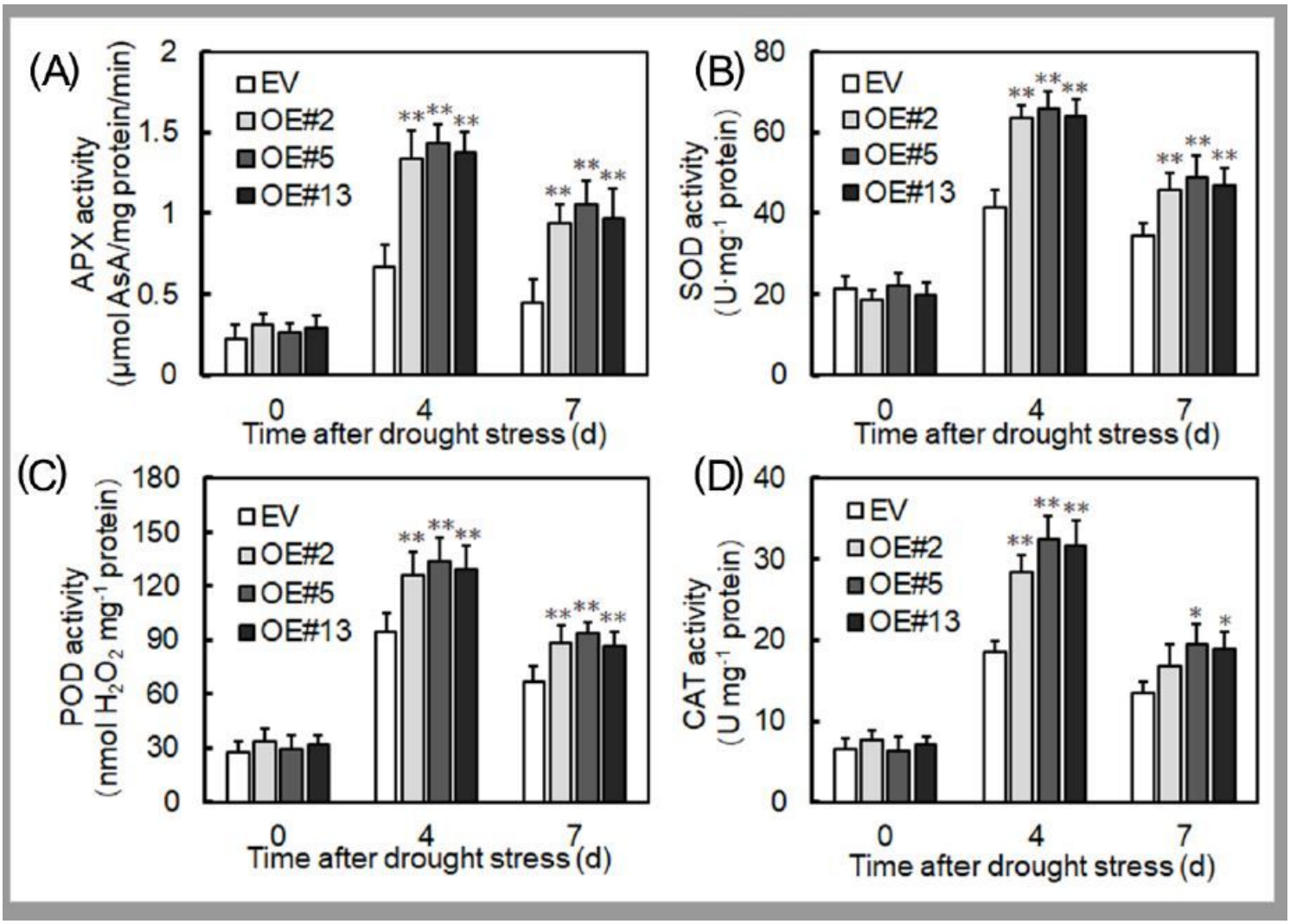

Figure 10

VyRCHC114-overexpressed and EV-transformed plants' activity of various antioxidant enzymes in Arabidopsis. a Under drought stress for 0, 4, and 7 days, are ascorbate peroxidase (APX), b superoxide dismutase (SOD), c peroxidase (POD), d catalase (CAT) activities of overexpressed (OE) and EV-transformed plants were determined. Data are mean ± SD (standard deviation). The asterisk, (*) and (**), indicates that OEs and EV-transformed groups were significantly different at $P < 0.05$ and $P < 0.01$ (Student's t-test).

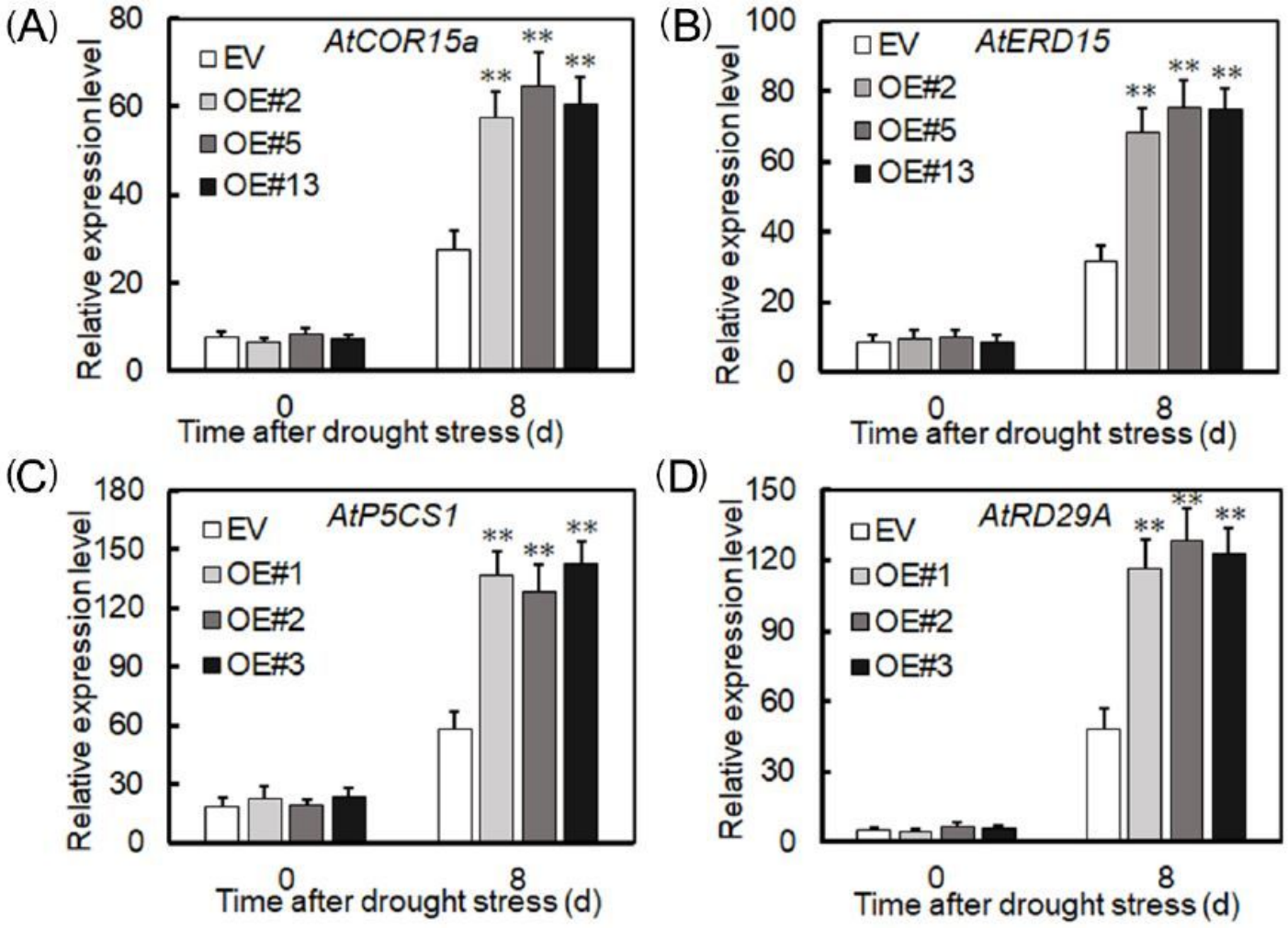

Figure 11

Relative expression levels of drought resistance genes in transgenic and EV-transformed Arabidopsis after drought stress. a AtCOR15a, b AtERD15, c AtP5CS1, d AtRD29A. Data are the mean ± SD (standard deviation). The asterisk, (*) and (**), indicates that overexpressed (OEs) and EV-transformed groups of plants were significantly different at $P < 0.05$ and $P < 0.01$ (Student's t-test).

Supplementary Files

This is a list of supplementary files associated with this preprint. Click to download.

- SupplementaryTable.xlsx
- SupplementaryFigure.docx
- Table3.xlsx
- Table1.xlsx
- Table2.xlsx